

Color and Texture Features for Image Indexing and Retrieval

Subrahmanyam Murala, Anil Balaji Gonde, R. P. Maheshwari

subbumurala@gmail.com, abgonde@gmail.com, rpmaheshwari@gmail.com

Department of Electrical Engineering, Indian Institute of Technology Roorkee,
Roorkee-247 667, Uttarakhand, India.

Abstract

The novel approach combines color and texture features for content based image retrieval (CBIR). The color and texture features are obtained by computing the mean and standard deviation on each color band of image and sub-band of different wavelets. The standard Wavelet and Gabor wavelet transforms are used for decomposing the image into sub-bands. The retrieval results obtained by applying color histogram (CH) + Gabor wavelet transform(GWT) to a 1000 image database demonstrated significant improvement in precision and recall, compared to the color histogram (CH), wavelet transform (WT), wavelet transform + color histogram (WT + CH) and Gabor wavelet transform (GWT).

1. Introduction:

Application of World Wide Web and the internet is increasing exponentially, and with it the amount of digital image data accessible to the users. A huge amount of Image databases are added every minute and so is the need for effective and efficient image retrieval systems. There are many features of content-based image retrieval but four [1] of them are considered to be the main features. They are colour, texture, shape, and spatial properties. Spatial properties, however, are implicitly taken into account so the main features to investigate are colour, texture and shape.

Two major approaches [1] including spatial and transform domain-based methods can be identified in (CBIR) systems. The first approach usually uses pixel (or a group of adjacent pixels) features like color and shape. Among all these features, color is the most used signature for indexing [2]. Color histogram [3] and its variations [4] were the first algorithms introduced in the pixel domain. In the second approach, transformed data are used to extract some higher-level features [5]. Wavelet-based (standard wavelets and Gabor wavelets) methods, which provide better local spatial information in transform domain have been used [6, 7]. In standard wavelets, Daubechies' wavelets are the most used in CBIR, because of their fast computation and regularity. In Ref. [8], Daubechies' wavelets in three scales were used to obtain transformed data. Then, histograms of wavelet coefficients in each sub-band were

computed and stored to construct indexing feature vectors. The Gabor wavelets are a group of wavelets, with each wavelet capturing energy at a specific frequency and a specific direction. Expanding a signal using this basis provides a localized frequency description, therefore capturing local features/energy of the signal. Texture features can then be extracted from this group of energy distributions. The scale (frequency) and orientation tunable property of Gabor filter makes it especially useful for constructing indexing feature vectors.

The main motivation of the present work is to use the texture feature in combination with color histograms, which yield improved performance. Through combination of different wavelets decomposition planes and histograms we can increase the number of features, which in turn improves the retrieval accuracy. To support the efficient and fast retrieval of similar images from image databases, feature extraction plays an important role in content-based image retrieval.

The organization of the paper is as follows. In section 2, a brief review of color histogram method is given. Section 3 presents a brief review of texture feature. In section 4, a feature extraction and similarity measurement are presented. Experimental results and discussion are given in section 5. Finally, conclusions are presented in section 6.

2. Color

In content based Image retrieval, color descriptor has been one of the first choices because if one chooses a proper representation, it can be partially reliable even in presence of changes in lighting, view angle, and scale. In image retrieval, the color histogram is the most commonly used global color feature. It denotes the probability of the intensities of the three color channels.

Typical characterization of color composition is done by color histograms. In 1991 Swain and Ballard [3] proposed the method, called color indexing, which identifies the object using color histogram indexing. The color histogram is obtained by counting the number of times each color occurs in the image array. Histogram is invariant to translation and rotation of the image

plane, and change only slowly under change of angle of view [3].

A color histogram H for a given image is defined as a vector

$$H = \{H[0], H[1], \dots, H[i], \dots, H[N]\} \quad (1)$$

Where i represent the color in color histogram and $H[i]$ represent the number of pixels of color i in the image, and N is the number of bins used in color histogram. For comparing the histogram of different sizes, color histogram should be normalized. The normalized color histogram is given as

$$H' = \frac{H}{p}$$

where p is the total number of pixels in the image. In this paper, RGB color space is used i.e. histogram for each color channel is used as feature for image database.

3. Texture

3.1 Standard Wavelet

The wavelet transform provides a multi-resolution approach to texture analysis and classification. Studies of human visual system support a multi-scale texture analysis approach, since researchers have found that the visual cortex can be modelled as a set of independent channels, each tuned to a particular orientation and spatial frequency band. That is why wavelet transforms are found to be useful for texture feature extraction.

The 1-D discrete wavelet transform (DWT) decomposes a signal $f(t) = L^2(R)$ in terms of shifted and dilated mother wavelet $\psi(t)$ and scaling function $\varphi(t)$ [9].

$$f(t) = \sum_{l \in Z} s_{j_0, l} \varphi_{j_0, l}(t) + \sum_{j \geq j_0} \sum_{l \in Z} w_{j, l} \psi_{j, l}(t) \quad (2)$$

Where $\varphi_{j_0, l}(t) = 2^{\frac{j_0}{2}} \varphi(2^{j_0} t - l)$ and $\psi_{j, l}(t) = 2^{\frac{j}{2}} \psi(2^j t - l)$. If $\{\varphi_{j_0, l}, \psi_{j, l} | j \geq j_0, l \in Z\}$ form an orthonormal basis of $L^2(R)$, then the scaling coefficients $s_{j_0, l}$ and wavelet coefficient $w_{j, l}$ can be calculated using the standard L^2 inner product: $s_{j_0, l} = \langle f, \varphi_{j_0, l} \rangle$ and $w_{j, l} = \langle f, \psi_{j, l} \rangle$.

An image is a 2-D signal. The DWT decomposes an image $f(x, y) = L^2(R^2)$ in terms of a set of shifted and dilated wavelet functions $\{\psi^{0^\circ}, \psi^{90^\circ}, \psi^{\pm 45^\circ}\}$ and scaling function $\varphi(x, y)$:

$$f(x, y) = \sum_{k \in Z^2} s_{j_0, k} \varphi_{j_0, k}(x, y) + \sum_{b \in \theta} \sum_{j \geq j_0} \sum_{k \in Z^2} w_{j, k}^b \psi_{j, k}^b(x, y) \quad (3)$$

$$\text{where } \varphi_{j_0, k}(x, y) = 2^{\frac{j_0}{2}} \varphi(2^{j_0} (x, y) - k),$$

$$\psi_{j, k}^b(x, y) = 2^{\frac{j}{2}} \psi^b(2^j (x, y) - k)$$

and $b \in \theta = \{0^\circ, 90^\circ, \pm 45^\circ\}$. The $0^\circ, 90^\circ$ and $\pm 45^\circ$ denote the sub bands of the wavelet decomposition. A separable 2-D discrete wavelet transform can be computed efficiently in discrete space by applying the associated 1-D filter bank to each column of the image, and then applying the filter bank to each row of the resultant coefficients. Fig.1 shows a three level pyramidal wavelet decomposition of an image $I = f(x, y)$ of size $a \times b$ pixels. In the first level of decomposition, one low pass sub image (S_1) and three orientation selective high pass sub images (w_1^H, w_1^V, w_1^D) are created. In second level of decomposition, the low pass sub image is further decomposed into one low pass and three high pass sub images (w_2^H, w_2^V, w_2^D). The process is repeated on the low pass sub image to form higher level of wavelet decomposition. In other words, DWT decomposes an image in to a pyramid structure of the sub images with various resolutions corresponding to the different scales. Three-stage decomposition will create three low pass sub images and nine (three each in horizontal, vertical, and diagonal direction) high pass directional sub images. The low pass sub images are low-resolution versions of the original image at different scales. The horizontal, vertical and diagonal sub images provide the information about the brightness changes in the corresponding directions respectively.

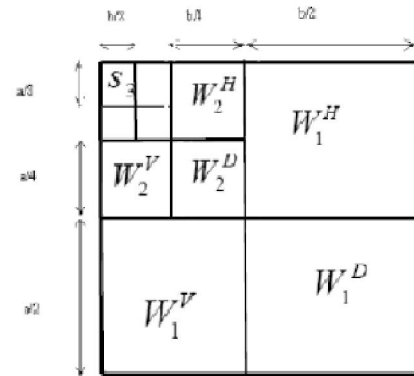


Fig.1: Standard Wavelet Decomposition.

3.2 Gabor Wavelet

A 2D Gabor function is a Gaussian modulated by a complex sinusoid. It can be specified by the frequency of the sinusoid ω and the standard

deviations σ_x and σ_y of the Gaussian envelope as follows [10]:

$$\psi(x, y) = \frac{1}{2\pi\sigma_x\sigma_y} e^{[-(1/2)(x^2/\sigma_x^2 + y^2/\sigma_y^2) + 2\pi j\alpha x]} \quad (4)$$

2D Gabor wavelets that satisfy the wavelet theory have been obtained as [11]:

$$\begin{aligned} \psi(\omega, \theta, x, y) &= \frac{\omega}{\sqrt{2\pi k}} e^{[-(\omega^2/8k^2)(4(x\cos\theta+y\sin\theta)^2 + (-x\sin\theta+y\cos\theta)^2)]} \\ &\times [e^{j(\omega x\cos\theta+\omega y\sin\theta)} - e^{(-k^2/2)}], \end{aligned} \quad (5)$$

Where ω the radial frequency in radians per unit length and θ is the wavelet orientation in radians. The Gabor wavelet is centred at $(x=0, y=0)$ and the normalization factor is such that $\langle \psi, \psi \rangle = 1$, i.e. normalized by L^2 norm. k is a constant, with $k \approx \pi$ for a frequency bandwidth of one octave and $k \approx 2.5$ for a frequency bandwidth of 1.5 octaves. It has been demonstrated that the 2D Gabor functions are local spatial band pass filters that achieve the theoretical limit for conjoint resolution on information in the 2D spatial and 2D Fourier domains [10]. Examples of Gabor wavelets according to Eq. (5) are shown in Fig. 2 [11].

Gabor functions do not result in an orthogonal decomposition [11], which means that a wavelet transform based upon the Gabor wavelet is redundant. Manjunath and Ma [12] proposed a design strategy to project the filters so as to ensure that the half-peak magnitude supports of the filter responses in the frequency spectrum touch one another. By doing this, it can be ensured that the filters will capture the maximum information with minimum redundancy [13].

The Gabor wavelets are obtained by dilation and rotation of the generating function $\psi(x, y)$ as follows:

$$\psi_{mn}(x, y) = a^{-m}\psi(x', y'), \quad (6)$$

where $x' = a^{-m}(x\cos\theta + y\sin\theta)$

$$y' = a^{-m}(-x\sin\theta + y\cos\theta)$$

$$\theta = n\pi/K,$$

$m \in \{0, \dots, S-1\}$ and $n \in \{0, \dots, k-1\}$, represent scale and orientation, respectively; and K and S are the number of desired orientations and scales, respectively.

The variables in the above equations are defined as follows:

$$a = (U_h/U_l)^{\frac{1}{M-1}}, \quad \omega_{m,n} = U_h$$

$$\sigma_{x,m,n} = \frac{(a+1)\sqrt{2\ln 2}}{2\pi a^m(a-1)U_l}$$

$$\sigma_{y,m,n} = \frac{1}{2\pi \tan(\frac{\pi}{2N}) \sqrt{\frac{U_h^2}{2\ln 2} - (\frac{1}{2\pi\sigma_{x,m,n}})^2}}$$

The response of Gabor filter is the convolution of Gabor window with image I is given by

$$G_{mn}(x, y) = \sum_s \sum_t I((x-s, y-t)) \psi_{mn}^*(s, t) \quad (7)$$

Where, U_h and U_l are the upper and lower bound of the designing frequency band, respectively.

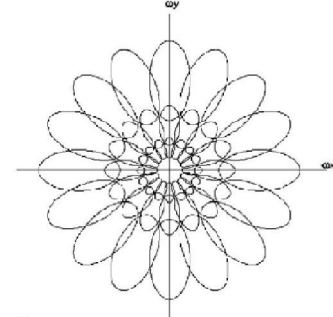


Fig.2: Gabor wavelets in the spatial frequency plane. Each ellipse shows the half-amplitude bandwidth contour dilated by a factor of 2, covering almost the complete support of a wavelet [11].

In this implementation, we used the following constants as commonly used in the literature:

$U_l = 0.05$, $U_h = 0.49$, s and t range from -30 to +30, i.e., filter mask size is 60×60 .

4. Feature Extraction

4.1 Color Histogram

In this paper 64 bins are used for each color channel. Totally we obtain 192 features for each image. These 192 features are used for feature vector calculation.

4.2 Texture

A. Wavelet Transform

After applying the 2D-wavelet transform of 3 scales, we obtain array of 12 sub-bands. Finally obtain the mean μ_m and standard deviation σ_m for each sub-band.

$$\begin{aligned} \mu_m &= \sum_x \sum_y W_m(x, y), \text{ and} \\ \sigma_m &= \sqrt{\sum_x \sum_y (|W_m(x, y)| - \mu_m)^2} \end{aligned} \quad (8)$$

A feature vector f is given by:

$$f = (\mu_1, \mu_2, \dots, \mu_{12}, \sigma_1, \sigma_2, \dots, \sigma_{12}). \quad (9)$$

B. Gabor Wavelet Transform

After applying Gabor filters on the image with different orientation at different scale, we obtain an array of magnitudes. The main purpose of texture-based retrieval is to find images or regions with similar texture. It is assumed that we are interested in images or regions that have homogenous texture, therefore the following mean μ_{mn} and standard deviation σ_{mn} of the magnitude of the transformed coefficients are used to represent the homogenous texture feature of the region:

$$\mu_{mn} = \sum_x \sum_y G_{mn}(x, y), \text{ and}$$

$$\sigma_{mn} = \sqrt{\sum_x \sum_y (|G_{mn}(x, y)| - \mu_{mn})^2}$$

A feature vector f (texture representation) is created using μ_{mn} and σ_{mn} as the feature components [12]. Three scales and four orientations are used in common implementation and the feature vector is given by:

$$f = (\mu_{00}, \mu_{01}, \dots, \mu_{23}, \sigma_{00}, \sigma_{01}, \dots, \sigma_{23}). \quad (10)$$

4.3 Proposed Method

The novel method of GWT+CH gives best results compared to color histogram, wavelet transform, wavelet transform + color histogram and Gabor wavelet.

4.4 Image Database

The database used in the experimentation consists of 10 different groups, and each group consists of 100 images from Correl database. All these images in the database are natural images.

4.5 Similarity Measure

A query image is any one of 1000 images from image database. This image is processed to compute features with different wavelets and histograms on color bands. Then d_1 distance metric given by Eq. (11) is used to compute the similarity or match value for given pair of images.

$$D(Q, T) = \sum_{i=1}^{\Gamma} \frac{|Q_i - T_i|}{1 + Q_i + T_i} \quad (11)$$

Where Q_i is feature vector of query image, T_i is feature vector of image database and Γ is the feature vector length.

5. Experimental Results

For evaluation of the proposed method, some query images were selected randomly from a 1000 image subset of the COREL database. The images in the database have different sizes and are categorized in 10 classes as listed in Tables (a) and

(b). Each class contains 100 pictures in JPEG format. Within this database, it is known whether any two images are of the same category. In particular, a retrieved image is considered a match if and only if it is in the same category as the query. This assumption is reasonable, since the 10 categories were chosen so that each depicts a distinct semantic topic. Fig. 4 illustrates four query results of our indexing-retrieval program developed based on the GWT+CH. Each query results in a preselected number of retrieved images which are illustrated and listed in ascending order according to the d_1 distance between indexing vectors of the query and retrieved images.

The novel approach of GWT + CH is compared with WT, WT + CH and GWT in terms of average precision, and recall. Precision (P), and recall (R) for query image I_k ($k = 1, \dots, 1000$) are defined as:

$$P(I_k, N) = \frac{\text{No. of relevant images retrieved}}{\text{Total No. of images retrieved}(N)} \quad (12)$$

$$R(I_k) = P(I_k, |A(I_k)|) \quad (13)$$

Where, $|A(I_k)|$ represents the numbers of relevant images in the respective category. The average precision for images belonging to the q^{th} category (A_q) has been computed by [1]:

$$\bar{P}_q = \sum_{k \in A_q} P(I_k) / |A_q|, q = 1, 2, \dots, 10. \quad (14)$$

Finally, the average precision is given by:

$$\bar{P} = \sum_{q=1}^{10} \bar{P}_q / 10 \quad (15)$$

The average recall is also computed in the same manner. As shown in Fig.3, Tables (a) and (b), the proposed method performed better than CH, WT, WT + CH and GWT in terms of all of the above evaluation measures.

6. Concluding Remarks

In this paper, a novel approach called Gabor wavelet transform + color histogram in CBIR is presented. Simulation results demonstrated higher performance of the proposed method compared to the WT + CH and GWT in terms of average precision and recall. The performance of the proposed method can be improved by applying the same low level features on region based image retrieval.

Table (a): Results of novel approach Wavelet transform is compared with color histogram and wavelet transform.

S. No:	Category	Color Histogram		Wavelet Transform		Color Histogram + Wavelet Transform	
		\bar{P} % (N=10)	\bar{R} %	\bar{P} % (N=10)	\bar{R} %	\bar{P} % (N=10)	\bar{R} %
1	Africans	73.00	38.50	37.10	16.08	75.60	39.18
2	Beaches	49.20	24.33	24.20	19.75	50.10	24.62
3	Buildings	46.00	19.13	29.80	12.42	47.40	19.47
4	Buses	46.15	32.72	57.20	34.65	50.20	35.55
5	Dinosaurs	99.25	96.02	75.21	45.09	100.0	98.01
6	Elephants	58.10	28.21	39.40	20.10	60.19	25.73
7	Flowers	75.15	40.15	46.16	34.27	76.21	42.16
8	Horses	89.20	38.02	35.20	20.83	89.10	42.17
9	Mountains	27.17	14.77	28.12	22.54	29.10	15.35
10	Food	59.15	25.90	35.25	23.88	60.70	26.38
	Total	62.20	35.70	40.76	24.96	63.80	36.80

Table (b): Results of novel approach Gabor Wavelet transform is compared with color histogram and Gabor wavelet transform.

S. No:	Category	Color Histogram		Gabor Transform		Color Histogram + Gabor Transform	
		\bar{P} % (N=10)	\bar{R} %	\bar{P} % (N=10)	\bar{R} %	\bar{P} % (N=10)	\bar{R} %
1	Africans	73.00	38.50	32.20	17.37	75.90	39.20
2	Beaches	49.20	24.33	28.80	18.08	50.00	24.72
3	Buildings	46.00	19.13	28.90	12.88	46.80	19.34
4	Buses	46.15	32.72	35.12	29.48	51.70	36.00
5	Dinosaurs	99.25	96.02	80.19	55.14	100.0	99.00
6	Elephants	58.10	28.21	40.15	25.80	61.70	28.65
7	Flowers	75.15	40.15	63.30	43.53	79.50	43.69
8	Horses	89.20	38.02	38.10	16.00	90.80	43.70
9	Mountains	27.17	14.77	31.60	17.25	28.40	15.1
10	Food	59.15	25.90	33.70	18.60	62.80	26.35
	Total	62.20	35.70	41.20	25.41	64.76	37.50

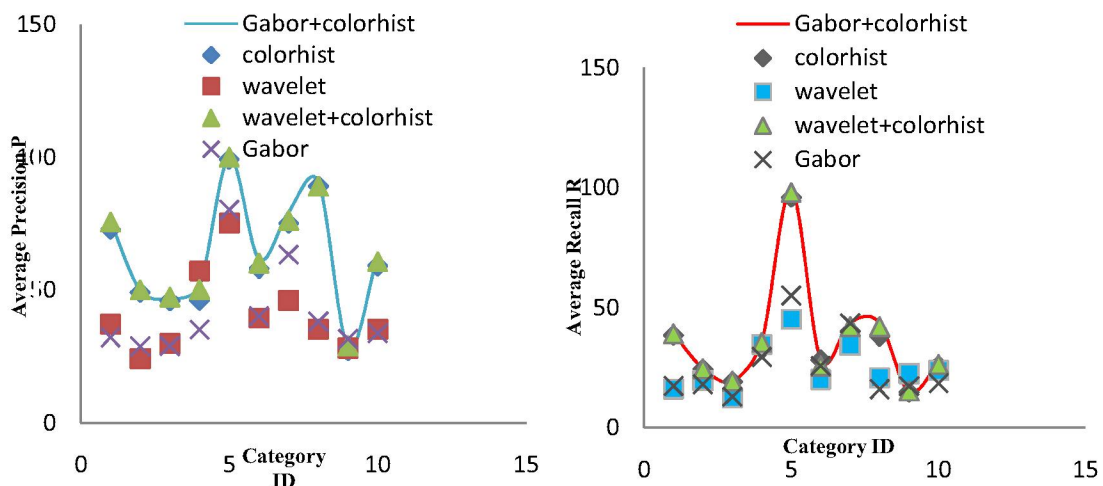


Fig.3: Comparing the proposed method with the color histogram, wavelet transform, wavelet transform + color histogram and Gabor wavelet transform methods on average precision(P) and average recall(R).

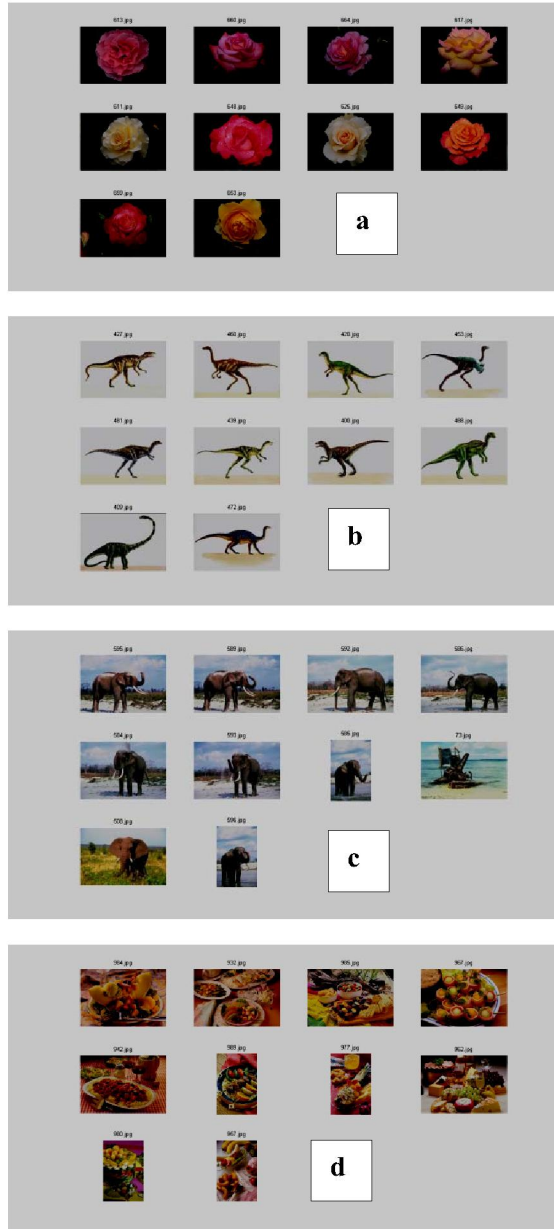


Figure.4: Results obtained for query images (a) 613, (b) 427, (c) 595, (d) 984 of proposed method

References

- [1] H. Abrishami-Moghadam, T. Taghizadeh Khajoie, A. H.Rouhi, M. Saadatmand-T., Wavelet correlogram: a new approach for image indexing and retrieval, *J. Elsevier Pattern Rec.* 38 (2005) 2506 – 2518
- [2] Th. Gevers, in: M. Lew (Ed.), *Color Based Image Retrieval, Multimedia Search*, Springer, Berlin, 2001.
- [3] M.J. Swain, D.H. Ballard, Color indexing, *Int. J. Comput. Vis.* 7 (1991) 11–32.
- [4] M. Flickner, H. Sawhney, W. Niblack, J. Ashley, Q. Huang, B. Dom, M. Gorkani, J. Hafner, D. Lee, D. Petkovic, D. Steele, P. Yanker, Query by image and video content: the QBIC system, *IEEE Comput.* 28 (9) (1995) 23–32.
- [5] L. Balmelli, A. Mojsilovic, *Wavelet Domain Features for Texture Description, Classification and Replicability Analysis, Wavelets in Signal and Image Analysis: From Theory to Practice* (edited book), Kluwer Academic Publishers, Netherland, 2001.
- [6] J. Li, J.Z. Wang, G. Wiederhold, SIMPLIcity: semanticssensitive integrated matching for picture libraries, *IEEE Trans. Pattern Anal. Mach. Intell.* 23 (9) (2001) 947–963.
- [7] J.Z. Wang, G. Wiederhold, O. Firschein, S.X. Wei, Content based image indexing and searching using Daubechies' wavelets, *Int. J. Digital Libraries* 1 (4) (1998) 311–328.
- [8] M.K. Mandal, S. Panchanathan, T. Aboulnasr, Fast wavelet histogram techniques for image indexing, *J. Comput. Vis. Image Understanding* 75 (1/2) (1999) 99–110.
- [9] M.B Kokare, *Wavelet Based Features for Texture Image Retrieval*, Ph.D. Thesis, IIT, Kharagpur, Chapter 2, pp 15-35, 2004.
- [10] J.G. Daugman, Uncertainty relation for resolution in space, spatial frequency, and orientation optimized by two dimensional visual cortical filters, *J. Opt. Soc. Am. 2* (7) (1985) 1160–1169.
- [11] T.S. Lee, Image representation using 2D Gabor wavelets, *IEEE Trans. Pattern Anal. Mach. Intell.* 16 (10) (1996) 959–971.
- [12] B.S. Manjunath, W.Y. Ma, Texture features for browsing and retrieval of image data, *IEEE Trans. Pattern Anal. Mach. Intell.* 18 (8) (1996) 837–842.
- [13] R.J. Ferrari, R.M. Rangayyan, J.E.L. Desautels, A.F. Frère, Analysis of asymmetry in mammograms via directional filtering with Gabor wavelets, *IEEE Trans. Med. Imaging* 20(9) (2001) 953–964.